Intramolecular, Intermolecular, and Heterogeneous Nonadiabatic Dissociative Electron Transfer to Peresters

Sabrina Antonello,[†] Fernando Formaggio,[‡] Alessandro Moretto,[‡] Claudio Toniolo,[‡] and Flavio Maran*,[†]

Contribution from the Department of Physical Chemistry, University of Padova, via Loredan 2, 35131 Padova, Italy, and the Biopolymer Research Center, C.N.R., Department of Organic Chemistry, University of Padova, via Marzolo 1, 35131 Padova, Italy

Received March 28, 2001

Abstract: The electron transfer to peresters was studied by electrochemical means in *N*,*N*-dimethylformamide. The reduction was carried out by three independent methods: (i) heterogeneously, by using glassy carbon electrodes, (ii) homogeneously, by using electrogenerated radical anions as the donors, and (iii) intramolecularly, by using purposely synthesized donor−spacer−acceptor (D-Sp-A) systems. Convolution analysis of the heterogeneous data led to results in excellent agreement with the dissociative electron transfer theory. The homogeneous redox catalysis data also confirmed the reduction mechanism. The cyclic voltammetries of the D-Sp-A molecules could be simulated, leading to determination of the corresponding intramolecular dissociative rate constants. Analysis of the results showed that, regardless of the way by which the acceptor is reduced, the investigated dissociative electron transfers are strongly nonadiabatic and, particularly, that the experimental rates are several orders of magnitude smaller than the adiabatic limit. A possible mechanism responsible for the observed behavior is discussed.

In the last 15 years the study of intramolecular electron transfer (ET) reactions in D-Sp-A molecules, in which a donor (D) and an acceptor (A) are separated by a molecular spacer (Sp), has provided a variety of information on how electrons are transferred through bonds and space.[1] Conversely, almost nothing is known about dissociative electron transfers (DETs), i.e., those reactions in which ET and bond cleavage are concerted.[2−4] Indeed, there is a relatively large amount of studies on the decay of radical anions occurring by fragmentation of a σ bond.[2,4,5] In most cases, however, the mixing of the π^* (donor side) and σ^* (acceptor side) orbitals is so strong that analysis of the rate data, e.g., in terms of the relevant thermodynamic parameters, may require several approximations. In fact, it has been argued that describing the reductive cleavage of these systems in terms of electron uptake followed by intramolecular transfer from the π^* orbital to the σ^* orbital is not a realistic model.[6] Generally speaking, the study of intramolecular ET processes, whether dissociative or not, is best performed by using systems in which the D and A functional moieties are spatially separated. Very recently, as a first step in this direction, we reported data on the ΔG° dependence of intramolecular DETs, using systems in which A was C−Br, D was a series of ring-substituted benzoates, and Sp was cyclohexyl.[7] The intramolecular rate constants were found to be more sensitive to variation of ΔG° than the corresponding intermolecular data. This was attributed to the substituent-dependent variation of the effective distance between the orbitals involved in the transfer. Concerning the distance effect caused by variation of the spacer's length, we expect the rate to decrease with distance along similar lines as reported for a variety of nondissociative systems. This is because of reduced electronic coupling between the reactant and product states, leading to nonadiabatic processes. In fact, there are some interesting results on the dissociative electron attachment to chloronorbornenes in which the efficiency of chloride ion production was related to the electronic coupling between localized C−Cl σ^* and C=C π^* orbitals.[8] Some data on the intramolecular DET in D-Sp-A systems in which Sp is a variable-length alkyl chain have also been reported.[9] The absence of rigidity in the investigated molecules appears to be responsible for the small distance effect on the intramolecular DET rates. The role of orbital symmetry restrictions on the efficiency of π^*/σ^* coupling has been stressed for the intramolecular reduction of halides.[8a,10] Besides distance or symmetry effects, however, we obtained some evidence

* Corresponding author: (tel) +39 (049) 827-5147; (fax) +39 (049) 827-5135; (e-mail) f.maran@chfi.unipd.it.

[†] Department of Physical Chemistry.

[‡] Department of Organic Chemistry.

(1) For example, see: (a) Closs, G. L.; Miller, J. R. *Science* **1988**, *240*, 440. (b) Paddon-Row, M. N. *Acc. Chem. Res.* **1994**, *27*, 18. (c) *Electron Transfer−From Isolated Molecules to Biomolecules*; Jortner, J., Bixon, M., Eds.; Wiley: New York, 1999; Part 1.

(2) (a) Savéant, J.-M. In *Advances in Electron-Transfer Chemistry*; Mariano, P. S., Ed.; JAI Press: Greenwich, CT, 1994; Vol. 4, p 53. (b) Savéant, J.-M. *Adv. Phys. Org. Chem.* **2000**, *35*, 117.

(3) Eberson, L. *Acta Chem. Scand.* **1999**, *53*, 751.

(4) Maran, F.; Wayner, D. D. M.; Workentin, M. S. *Adv. Phys. Org. Chem.* **2001**, *36*, in press.

(5) (a) Maslak, P. In *Topics in Current Chemistry*; Mattay, J., Ed.; Springer-Verlag: Berlin, 1993; Vol. 168, p 1. (b) Savéant, J.-M. *J. Phys. Chem.* **1994**, *98*, 3716.

(6) Burrow, P. D.; Gallup, G. A.; Fabrikant, I. I.; Jordan, K. D. *Austr. J. Phys.* **1996**, *49*, 403.

(7) Antonello, S.; Maran, F. *J. Am. Chem. Soc.* **1998**, *120*, 5713.

(8) (a) Pearl, D. M.; Burrow, P. D.; Nash, J. J.; Morrison, H.; Jordan, K. D. *J. Am. Chem. Soc.* **1993**, *115*, 9876. (b) Pearl, D. M.; Burrow, P. D.; Nash, J. J.; Morrison, H.; Nachtigallova, D.; Jordan, K. D. *J. Phys. Chem.* **1995**, *99*, 12379.

(9) (a) Kimura, N.; Takamuku, S. *Bull. Chem. Soc. Jpn.* **1991**, *64*, 2433. (b) Kimura, N.; Takamuku, S. *Bull. Chem. Soc. Jpn.* **1992**, *65*, 1668. (c) Kimura, N.; Takamuku, S. *J. Am. Chem. Soc.* **1995**, *116*, 4087. (d) Kimura, N.; Takamuku, S. *J. Am. Chem. Soc.* **1995**, *117*, 8023.

(10) Addock, W.; Andrieux, C. P.; Clark, C. I.; Neudeck, A.; Savéant, J.-M.; Tardy, C. *J. Am. Chem. Soc.* **1995**, *117*, 8285.

10.1021/ja010799u CCC: $20.00
Published on Web 09/01/2001

indicating that there can be kinetically slow intermolecular DETs, the homogeneous ET to the O−O bond of dialkyl peroxides,[11] for which poor electronic coupling is attributable to the nature of the acceptor itself.

We are currently studying the distance dependence of DETs and more generally the problem of nonadiabaticity by using different types of spacer to control the electronic interaction between the D and A redox moieties. Thus, we devised the D-Sp-A systems **1a,b** in which A is the dissociative-type *tert*-

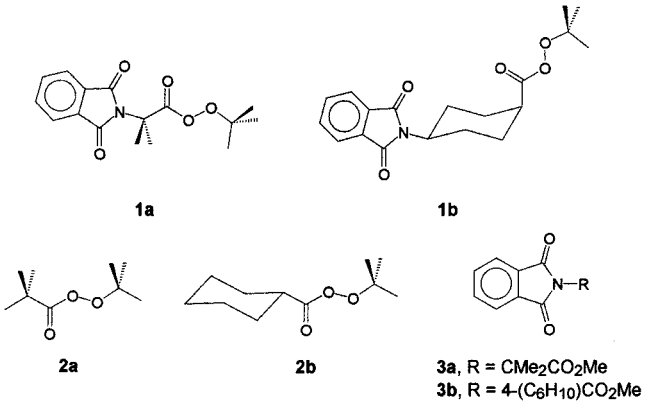

butyl perester function, CO_2-OtBu,[12] and Sp is a rigid molecular framework, CMe_2 and 1,4-cyclohexanediyl. In this paper, we describe the results that we obtained by studying the redox properties of **1a,b** and of the related molecules **2a,b** and **3a,b**. Data on the distance effect on the intramolecular DET rate are provided. Rate data are reported also for the heterogeneous and intermolecular reduction of the perester O−O bond. Analysis of the data led to discovery that regardless of the way by which the reaction is carried out, ET to the perester acceptor is an exceptionally slow DET.

Results and Discussion

Electroreduction of 2 and 3 and Analysis of the DET Mechanism. Models of both the acceptor (**2a,b**) and donor moieties (**3a,b**) were used to analyze, independently, their redox behavior both at the electrode and in the bulk. The experiments were carried out in DMF/0.1 M Bu_4NClO_4 (TBAP) at 25 °C. The electrode reduction of model peresters **2a** and **2b** was studied by cyclic voltammetry. Both reductions are characterized by an irreversible and broad peak (at 0.2 V s^{-1}, the peak potential, E_p, values of **2a** and **2b** are −1.55 and −1.50 V, respectively), in agreement with the voltammetric behavior expected for heterogeneous processes controlled by the activation barrier. The dependence of the normalized peak current, $i_p/v^{1/2}$, on the scan rate v is illustrated for **2a** in Figure 1. The decrease of $i_p/v^{1/2}$ together with the fact that the peak broadens when v increases indicate that the electron-transfer coefficient α depends on the applied potential E.[12−14] Convolution analysis

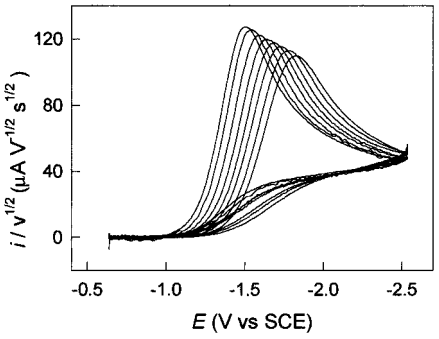

Figure 1. Background-subtracted cyclic voltammetries for the reduction of 2.1 mM **2a** in DMF−0.1 M TBAP at 25 °C. Left to right: 0.1, 0.2, 0.5, 1, 2, 5, 10, 20 V s^{-1}.

was thus carried out to study in detail the kinetics of the heterogeneous reduction.[4,12,13,15] The $i-E$ curves were transformed into the corresponding convolution current (I) versus E curves, leading to plots of excellent quality (independence, within 1−2%, of the limiting value of I on v).[16] In the convolution analysis, the i and I values are then combined to obtain the potential dependence of both the heterogeneous rate constant, k_{het}, and the transfer coefficient α.[17] By applying the basic concepts of the Savéant DET model,[18] the standard potential ($E°$) of the dissociative reduction of the perester was estimated by calculating the value of E corresponding to $\alpha = 0.5$. This $E°$ value was then used to calculate the standard rate constant, $k°_{het}$. The intrinsic barrier of the DET ($\Delta G_0^{\neq}$) was obtained from the slope of the $\alpha-E$ plot.[13,18] The consistency of the $E°$ and $k°_{het}$ values was finally checked by digital simulation of the cyclic voltammograms, which led to good reproduction of the experimental curves. For **2a**, the values of $E°$, $k°_{het}$, and $\Delta G_0^{\neq}$ are −0.30 V, 1×10^{-10} cm s^{-1}, and 12.2 kcal mol^{-1}, respectively. The corresponding values of **2b** are very similar, being −0.24 V, 9×10^{-11} cm s^{-1}, and 13.3 kcal mol^{-1}.

To check the actual reduction mechanism, we compared the results obtained with **2a** with those predicted by applying the DET theory.[17] The $E°$ of the concerted DET can be conveniently expressed through a thermochemical cycle[13] which, for the present case, is expressed as $E° = E°_{tBuCOO•/tBuCOO-} - BDFE/F$. BDFE is the bond dissociation free energy of the peroxide O−O bond. The $E°$ of the leaving group, $E°_{tBuCOO•/tBuCOO-}$, was estimated to be 0.82 V by analysis and simulation of the

(11) Donkers, R. L.; Maran, F.; Wayner, D. D. M.; Workentin, M. S. *J. Am. Chem. Soc.* **1999**, *121*, 7239.

(12) (a) Antonello, S.; Maran, F. *J. Am. Chem. Soc.* **1997**, *119*, 12595. (b) Antonello, S.; Maran, F. *J. Am. Chem. Soc.* **1999**, *121*, 9668.

(13) Antonello, S.; Musumeci, M.; Wayner, D. D. M.; Maran, F. *J. Am. Chem. Soc.* **1997**, *119*, 9541.

(14) Conventional analysis of electrochemically irreversible peaks should provide v-independent $i_p/v^{1/2}$ and peak width ($\Delta E_{p/2}$) values (For example, see: Bard, A. J.; Faulkner, L. R. *Electrochemical Methods, Fundamentals and Applications*, 2nd ed.; Wiley: New York, 2001.). This is because the Butler−Volmer description of electrode kinetics is employed, which implies that the transfer coefficient α is constant at any E values. As previously discussed in detail,[12,13,15b] the nonconstancy of α with respect to E fully accounts for experimental trends such as those here described.

(15) (a) Imbeaux, J. C.; Savéant, J.-M. *J. Electroanal. Chem.* **1973**, *44*, 169. (b) Savéant, J.-M.; Tessier, D. *J. Electroanal. Chem.* **1975**, *65*, 57.

(16) I and i are related by the convolution integral[15]

$$I = \pi^{-1/2} \int_0^t \frac{i(u)}{(t-u)^{1/2}}\,du$$

The sigmoidal $I - E$ curves are characterized by a diffusion-controlled limiting value $I_1 = nFAD^{1/2}C^*$, where n is the overall electron consumption, A the electrode area, D the diffusion coefficient, and C^* the substrate concentration. Provided the electrode process is irreversible, I and i are related to k_{het} through equation

$$\ln k_{het} = \ln D^{1/2} - \ln \{[I_1 - I(t)]/i(t)\}$$

Being $\alpha = -(RT/F)\partial \ln k_{het}/\partial E$, the apparent value of the transfer coefficient α can be experimentally determined as a function of E by derivatization of the $\ln k_{het}/D^{1/2} - E$ plots.

(17) Savéant, J.-M. *J. Am. Chem. Soc.* **1987**, *109*, 6788.

(18) (a) The DET model[17] leads to the same relationship between the activation free energy $\Delta G^{\neq}$ and free energy $\Delta G°$ obtained by Marcus for outer-sphere ETs (For example, see: Marcus, R. A.; Sutin, N. *Biochim. Biophys. Acta* **1985**, *811*, 265.); i.e., $\Delta G^{\neq} = \Delta G_0^{\neq}[1 + \Delta G°/4\Delta G_0^{\neq}]^2$. (b) Under electrochemical conditions and by neglecting the double-layer effect, the rate/driving force relationship becomes $\Delta G^{\neq} = \Delta G_0^{\neq}[1 + F(E - E°)/4\Delta G_0^{\neq}]^2$. Since α is $\partial \Delta G^{\neq}/\partial \Delta G° = -(RT/F)\,\partial \ln k_{het}/\partial E$, it follows that $\Delta G_0^{\neq} = F/(8\,\partial\alpha/\partial E)$.

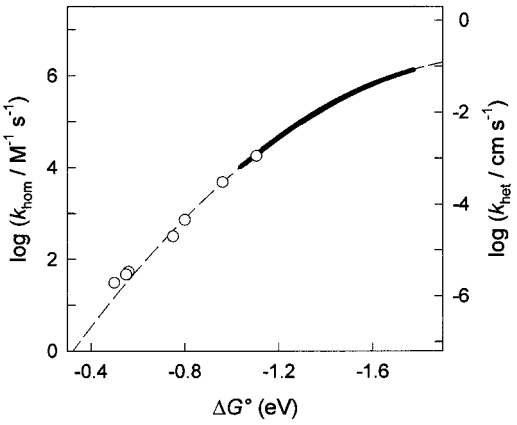

Figure 2. Comparison between homogeneous (○) and heterogeneous (•) rate constants for the reduction of pivaloyl peroxide **2a** in DMF at 25 °C. The dashed line is the second-order fit to the data (see text).

voltammetric oxidation peak of tBuCO$_2^-$, as previously described for other carboxylates.[12b,19,20] The bond dissociation energy (BDE) of **2a**, 30.6 kcal mol^{-1}, was corrected for the entropy by adding −6 kcal mol^{-1}.[21] $\Delta G_0^{\neq}$ was estimated through equation $\Delta G_0^{\neq} = (\mathrm{BDE} + \lambda_S)/4$,[17] where λ_S is the solvent reorganization energy. The latter was calculated to be 20.5 kcal mol^{-1} by using the empirical equation $\lambda_S = 55.7/r$,[13] where λ_S is given in kilocalories per mole and the molecular radius r in angstroms; r, 2.72 Å, was obtained by using the experimental diffusion coefficient and the Stokes−Einstein equation.[22] By using this procedure, we obtained for the concerted DET to **2a** the theoretical values $E° = -0.25$ V and $\Delta G_0^{\neq} = 12.8$ kcal mol^{-1}, in excellent agreement with the corresponding convolution results, −0.30 V and 12.2 kcal mol^{-1}.

The above analysis thus ensures that the reductions of **2a** and **2b** proceed by concerted ET/O−O bond cleavage (eq 1).

$$\mathrm{RCO_2{-}O}t\mathrm{Bu} + \mathrm{e} \rightarrow \mathrm{RCO_2}^- + t\mathrm{BuO}^{\bullet} \quad (1)$$

$$t\mathrm{BuO}^{\bullet} + \mathrm{e} \rightarrow t\mathrm{BuO}^- \quad (2)$$

The first reduction step is rapidly followed by the reduction of the tBuO$^{\bullet}$ radical (eq 2), which has $E° = -0.23$ V.[23] The reduction of the investigated peresters is also remarkably slow, $k°_{het}$ being 1×10^{-10} and 9×10^{-11} cm s^{-1} for **2a** and **2b**, respectively, which causes the peak to be more negative than the estimated $E°$ by ∼1.3 V. On the other hand, the reduction of the model donors is reversible (**3a**, $E° = -1.41$ V; **3b**, $E° = -1.45$ V) and fast (**3a**, $k°_{het}$(GC) = 0.13 cm s^{-1}, $k°_{het}$(Hg) = 0.12 cm s^{-1}; **3b**, $k°_{het}$(GC) = 0.12 cm s^{-1}), as expected for the formation of delocalized radical anions. In fact, convolution analysis of the reduction of **3a** gave evidence of a very small intrinsic barrier, which is consistent with a process ruled mainly by solvent reorganization. The analysis was carried out at low temperatures and relatively high scan rates to slow the heterogeneous kinetics. The data were thus obtained under conditions in which the ET is quasi-reversible.[15b] The temperature effect on $k°_{het}$, studied for **3a** in the range 233−278 K by using both mercury and glassy carbon electrodes, led to preexponential Arrhenius factor in the range $5 \times 10^2 - 5 \times 10^3$ cm s^{-1}, in agreement with an adiabatic outer-sphere ET.

Table 1. Reduction of **2a** by Radical Anions in DMF at 25°C

donor	$E°$ (V)	$\Delta G°$ (eV)	log k_{hom} (M^{-1} s^{-1})
3a	−1.41	−1.11	4.25
3-fluoro-**3a**	−1.26	−0.96	3.68
nitrobenzene	−1.10	−0.80	2.86
nitronaphthalene	−1.05	−0.75	2.50
4-nitroacetophenone	−0.86	−0.56	1.73
anthraquinone	−0.85	−0.55	1.67
4-nitrobenzonitrile	−0.80	−0.50	1.49

Homogeneous DET and Comparison with the Heterogeneous Results. The ET rate between free diffusing D and A was determined for **2a** by the homogeneous redox catalysis approach.[24] In this method, radical anion donors (D$^{-\bullet}$) are electrogenerated and used to reduce homogeneously the acceptor. Thus, the reversible reduction peak of the donor (or mediator) is transformed into a chemically irreversible, catalytic peak upon addition of the peroxide (eqs 3−5). The current of

$$\mathrm{D} + \mathrm{e} \rightleftarrows \mathrm{D}^{-\bullet} \quad (3)$$

$$\mathrm{D}^{-\bullet} + \mathrm{RCO_2{-}O}t\mathrm{Bu} \rightarrow \mathrm{D} + \mathrm{RCO_2}^- + t\mathrm{BuO}^{\bullet} \quad (4)$$

$$\mathrm{D}^{-\bullet} + t\mathrm{BuO}^{\bullet} \rightarrow \mathrm{D} + t\mathrm{BuO}^- \quad (5)$$

the catalytic peak depends on υ and the concentration of the acceptor. The rate constant (k_{hom}) values (Table 1) were determined by simulation of the experimental voltammograms obtained using scan rates in the range 0.2−2 V s^{-1} and at least three concentrations of the acceptor. Besides steps 3−5, the simulations included the set of side reactions already used for other peroxides.[11,23,25]

In Figure 2 the homogeneous and the heterogeneous ET data are combined together by adjusting the two vertical scales to fit the same parabola. The latter was generated by using the experimental heterogeneous $\Delta G_0^{\neq}$. Although the heterogeneous and the homogeneous $\Delta G_0^{\neq}$s are not exactly the same, the latter term can be estimated to be 11.5 kcal mol^{-1} and thus very similar to the heterogeneous one. The homogeneous $\Delta G_0^{\neq}$ was estimated as one-fourth of the sum of the BDE, 30.6 kcal mol^{-1},[21a] and the solvent reorganization energy λ_S, 15.4 kcal mol^{-1}. The λ_s value was estimated by using the empirical equation $\lambda_s = 95[(2r_D)^{-1} + (2r_A)^{-1} - (r_D + r_A)^{-1}]$,[11] where r_D and r_A are the donor and acceptor radii; an average value of 3.8 Å was used for r_D.[26] Therefore, by assuming the $\Delta G_0^{\neq}$ difference negligible, the difference between the two ordinates of Figure 2 would therefore reflect that between the two preexponential factors. The observed log Z_{hom} − log Z_{het} value,

(19) The oxidation peak of the carboxylate tBuCO$_2^-$ is characterized by the following parameters (0.2 Vs^{-1}): $E_p = 0.96$ V, peak width $\Delta E_{p/2} = 85$ mV, $\partial E_p/\partial \log \upsilon = 50$ mV/decade. The carboxylate was generated electrochemically through reduction of **2a** (eqs 1 and 2).

(20) Isse, A. A.; Gennaro, A.; Maran, F. *Acta Chem. Scand.* **1999**, *53*, 1013.

(21) (a) Bartlett, P. D.; Hiatt, R. R. *J. Am. Chem. Soc.* **1958**, *80*, 1398. (b) Theoretical calculations provided a very similar value, 31 kcal mol^{-1}: Benassi, R.; Taddei, F. *J. Mol. Struct.* **1994**, *303*, 101. (c) The entropy correction at 25 °C was estimated by taking into account both the commonly used fragmentation contribution (Benson, S. W. *Thermochemical Kinetics*, 2nd ed.; Wiley: New York, 1976.)[11] and the activation entropy for the thermal decomposition of **2a**.[21a]

(22) The diffusion coefficients of **2a** and **2b**, $D = 1.0 \times 10^{-5}$ and 9×10^{-6} cm^2 s^{-1}, respectively, were calculated from the limiting values of the convolution current.[16] Since the convolution analysis leads to $\ln(k_{het}/D^{1/2}) - E$ plots, these D values were also used to calculate the pertinent k_{het} and $k°_{het}$ values. The radius of **2a** was calculated also by using the effective radius approach[2a] or molecular models, leading to 2.64 and 2.59 Å, respectively; in either case, the increase of the value of λ_S is within 1 kcal mol^{-1}.

(23) Workentin, M. S.; Maran, F.; Wayner, D. D. M. *J. Am. Chem. Soc.* **1995**, *117*, 2120.

(24) (a) Andrieux, C. P.; Blocman, C.; Dumas-Bouchiat, J. M.; M'Halla, F.; Savéant J.-M. *J. Electroanal. Chem.* **1980**, *113*, 19. (b) Andrieux, C. P.; Savéant J.-M. *J. Electroanal. Chem.* **1986**, *205*, 43.

(25) Kjær, N. T.; Lund, H. *Acta Chem. Scand.* **1995**, *49*, 848.

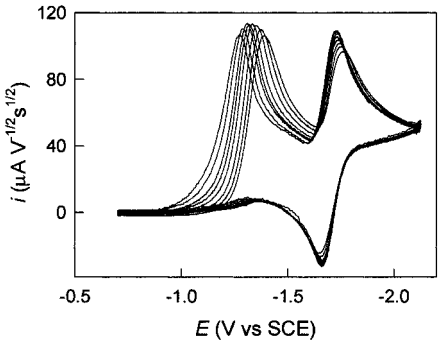

Figure 3. Background-subtracted cyclic voltammetries for the reduction of 2.3 mM **1a** in DMF−0.1 M TBAP at 25 °C. Left to right: 0.1, 0.2, 0.5, 1, 2, 5, 10, 20 V s^{-1}.

7.2, is indeed close to 7.8, the difference calculated by using the commonly accepted[2a,11,26a,27] *adiabatic* preexponential factors $Z_{hom} = 3 \times 10^{11}$ M^{-1} s^{-1} and $Z_{het} = 4.8 \times 10^3$ cm s^{-1} ($Z_{het} = (RT/2\pi M)^{1/2}$, where M is the molar mass of **2a**).

Because of their large intrinsic barriers, DETs are intrinsically slow ET processes. However, inspection of the data reveals that for the specific cases investigated both the k_{hom} and k_{het} values are *surprisingly small*. By using an Eyring-type rate constant expression ($k = Z' \exp(-\Delta G^{\neq}/RT)$, where Z' includes the transmission coefficient κ, i.e., $Z' = \kappa Z$), the quadratic DET rate/driving force relationship,[18a] the reaction free energy $\Delta G^\circ = -F(E^\circ_{\mathbf{2a}} - E^\circ_{D/D-\bullet})$, and the experimental k_{hom} values, the average Z'_{hom} results to be 1×10^6 M^{-1} s^{-1}. Even by considering[11] the latest modifications to the DET theory,[27] this value is still 4−5 orders of magnitude below the adiabatic limit. Therefore, we can conclude that the homogeneous DET to **2a** is strongly *nonadiabatic*, even more pronouncedly than previously observed with dialkyl peroxides such as di-*tert*-butyl peroxide and dicumyl peroxide.[11] Because of the empirical relationship between the homogeneous and the heterogeneous preexponential values that we commented on above, it follows that the electrode DET is also strongly nonadiabatic. In fact, by using the experimental k°_{het} and $\Delta G_0^{\neq}$ values of **2a**, we calculated $Z'_{het} = 0.1$ cm s^{-1}, a value that is almost 5 log units smaller than that expected for an adiabatic reduction. For **2b**, Z'_{het} is small as well, being 0.5 cm s^{-1}. These reductions are thus the first characterized cases of heterogeneous nonadiabatic DETs.

Intramolecular DET. The reduction of the D-Sp-A system **1a** exhibits an irreversible peak ($E_p = -1.29$ V, at 0.2 V s^{-1}) followed by a reversible component ($E^\circ = -1.70$ V). As verified in comparison with an authentic sample, the second peak is due to the reduction of the phthalimide moiety in the carboxylate anion D-Sp^-, formed together with *t*BuO$^\bullet$ in the DET. The dependence of the normalized peak current $i_p/v^{1/2}$ on v is illustrated in Figure 3. Although the figure is the equivalent of Figure 1, the pattern of the main reduction peak is pretty different. In fact, when v is progressively increased, $i_p/v^{1/2}$ first increases and then decreases.[28] At the same time, the peak first sharpens and then broadens; representative values of the peak width $\Delta E_{p/2}$ are 99, 78, and 99 mV at 0.1, 2, and 50 V s^{-1},

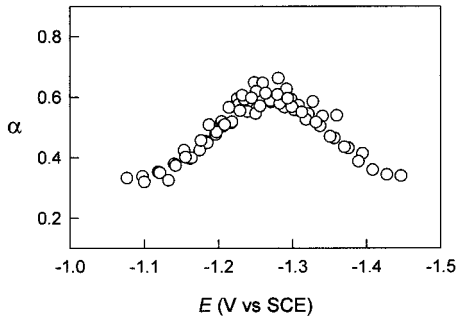

Figure 4. Potential dependence of α for the reduction of **1a** in DMF−0.1 M TBAP at 25 °C.

respectively. Convolution analysis of the first peak data led to evidence of a wavelike potential dependence of α (Figure 4), which is very similar to those previously reported for the reduction of some ring-substituted perbenzoates.[12] This is, in fact, the typical α−*E* pattern predicted for a DET occurring by mixed concerted/stepwise mechanism (eqs 6 and 7).[12b] Reaction

$$\text{D-Sp-A} + e \rightarrow \text{D-Sp}^- + \text{A}^\bullet \quad (6)$$

$$\text{D-Sp-A} + e \rightleftarrows {}^{\bullet-}\text{D-Sp-A} \rightarrow \text{D-Sp}^- + \text{A}^\bullet \quad (7)$$

6 corresponds to the direct reduction of the *slow end* (A) of the system (concerted DET). Conversely, reaction sequence 7 corresponds to electron injection into the *fast end* (D), followed by intramolecular DET from D to A (stepwise DET). The second mechanism has been discussed in detail for both dissociative-[7] and nondissociative-[29] type acceptors. In graphs a and b of Figure 5, the experimental curves and those simulated for the pathways 6 and 7 are compared for two different scan rates. It is evident that the first peak arises from the overlapping of the two components. On the other hand, because of the very different intrinsic barriers involved, the stepwise pathway is favored over the concerted DET at larger driving forces and thus when E becomes more negative.[2a,12] Since the peak is irreversible and thus scan rate dependent, the concerted-to-stepwise mechanism transition is conveniently induced by increasing v, as illustrated very nicely in graphs a and b of Figure 5. The practical result is that for E values more negative than −1.3 V the mechanism is essentially a pure stepwise process. As such, the α values obtained for $E < -1.3$ V should reflect the dependence on E typical of the fast end of **1a**. In fact, the slope estimated in this E region (cf. Figure 4) is in good agreement with that expected for an outer-sphere ET process ruled solely by solvent reorganization and is essentially the same of that obtained with the model donor **3a**.

Full simulation of the competitive mechanisms 6 and 7 is illustrated in graph c of Figure 5. The simulations of Figure 5 were carried out by using the information obtained with **2** and **3** and by taking into account the possible intermolecular side reactions, as described in detail elsewhere.[7,29] Because of the presence of the very short spacer $-CMe_2-$ (poor spatial separation between D and A) and the fact that **2a** has no amino substituents α to the carbonyl, the optimized E° values of the A and D ends of **1a** are 0.18 and 0.06 V more positive than those of **2a** and **3a**, respectively. For **1a,** the intramolecular rate constant (k_{intra}) was thus estimated to be 1.3×10^4 s^{-1}. The corresponding preexponential factor (Z'_{intra}) was calculated from k_{intra} and the quadratic DET rate/driving force relationship. The intrinsic barrier was obtained by considering that the O−O BDE

(26) (a) Kojima, H.; Bard, A. J. *J. Am. Chem. Soc.* **1975**, *97*, 6317. (b) Eberson, L. *Adv. Phys. Org. Chem.* **1982**, *18*, 79.

(27) Andrieux, C. P.; Savéant, J.-M.; Tardy, C. *J. Am. Chem. Soc.* **1998**, *120*, 4167.

(28) The small decrease of the $i_p/v^{1/2}$ ratio of the second peak is related to the relatively slow reduction of the carboxylate. In fact, the reduction of the phthalimide moiety in the carboxylate D-Sp^- has $k^\circ_{het} = 0.055$ cm s^{-1}, as determined by the Nicholson method (Nicholson, R. S. *Anal. Chem.* **1965**, *37*, 1351).

(29) Zheng, Z.-R.; Evans, D. H. *J. Am. Chem. Soc.* **1999**, *121*, 2941.

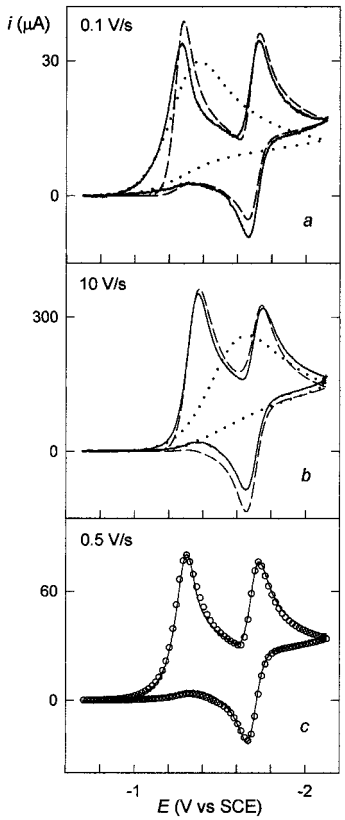

Figure 5. Comparison between background-subtracted cyclic voltammetries (solid lines) for the reduction of 2.3 mM **1a** at different scan rates, in DMF−0.1 M TBAP at 25 °C, and corresponding simulations. In graphs a and b, the curves were simulated by considering either the concerted (eq 6, dotted lines) or the stepwise (eq 7, dashed lines) mechanism. For clarity, the second peak was not included in the simulation of the concerted mechanism. Graph c illustrates the result of full simulation (○) of a typical experimental curve.

of **1a** is essentially the same of that of **2a**[30] and by taking into account, as previously described,[7] that the presence of the spacer increases the D/A distance and thus the solvent reorganization term.[1a] The experimental Z'_{intra} was thus estimated to be ∼7 orders of magnitude lower than the adiabatic limit $Z_{intra} = k_BT/h$. Although this difference includes some distance effect brought about by the short spacer, this finding points, once again, to the remarkable intrinsic slowness of the perester reduction.

The voltammetric behavior of **1b** is quite similar to that of **1a**. The main difference is that the reduction of D-Sp$^-$ is now easier ($E^\circ = -1.50$ V) because the cyclohexyl spacer of **1b** greatly diminishes the effect caused by the charge of the carboxylate on the E° of D. Simulation of the experimental curves, carried out as for **1a**, led to $k_{intra} = 2 \times 10^3$ s^{-1}. As expected for a system in which the spacer is sufficiently long to separate efficiently the electron exchanging moieties, the A and D groups are now characterized by the same E° values determined with the models **2b** and **3b**.

Although the k_{intra} of **1b** is smaller than that of **1a**, as expected, the decrease appears to be somewhat small compared to nondissociative-type systems.[1] This relatively small distance effect is not caused by a significant difference between the two DET driving forces, which are 1.23 and 1.20 eV for **1a** and **1b**, respectively. On the other hand, the spacer of **1a** is probably too short to put much weight on this comparison. We are currently investigating this aspect,[31] which is complicated by the fact that the relative D/A orientations of **1a** and **1b** seem to be significantly different. In fact, all other factors being the same, the strength of the π^*/σ^* coupling and thus k_{intra} depends not only on the separation but also on the relative orientation of the D and A groups. Concerning **1a** and **1b**, we drawn this preliminary conclusion by comparing the X-ray crystal structure of **1b**[32] with a molecular model of **1a**, built according to the X-ray structure of a similar molecule, α-(phthalimido)isobutyric anhydride.[33] The result obtained with **1b**, however, allows us to make another useful comparison with previous work. It is worth noting that the k_{intra} of **1b** is 2.2 orders of magnitude *smaller* than that of a bromide system of similar geometry, i.e., *cis*-1-methyl-4-benzoyloxycyclohexyl bromide, in which analogously to **1b**[32] the donor is equatorial and the acceptor axial, and driving force $\Delta G^\circ = -1.21$ eV, $\log k_{intra} = 5.5$.[7] This result would be surprising on the basis of a simple comparison between the two nuclear factors because the C−Br bond of tertiary alkyl bromides is ∼35 kcal mol^{-1} stronger than the O−O bond of peresters and thus the bromides have much larger intrinsic barriers than peroxides. Therefore, since the DET to tertiary alkyl bromides is adiabatic, as checked[11] by applying the nonadiabatic DET theory,[34] the observed small k_{intra} of **1b** also points to the remarkable slowness of perester reduction.

Nonadiabatic DET and Conclusions. The nonadiabaticity issue is emerging as an important but also intriguing aspect of DETs. Previously, we found that the homogeneous reduction of dialkyl peroxides is slower than expected on the basis of the adiabatic DET theory by ∼2 orders of magnitude.[11] More specifically, we used the nonadiabatic DET theory[34] and found that for these peroxides the electronic coupling energy between the reactant and product states, H_{RP}, is of the order of 15 cm^{-1}, a value distinctly below the commonly accepted adiabatic limit of 200 cm^{-1} ($\approx RT$).[35] In another study,[12b] we found that in order to account for the heterogeneous reduction kinetics of some ring-substituted perbenzoates, which proceeds by a competitive concerted/stepwise mechanism (cf. eqs 6 and 7), it was necessary to assume that the preexponential factor of the concerted DET component is ∼2 orders of magnitude smaller than that for the transient formation of the radical anion. In addition, by using our previous convolution results on, for example, the reduction of *tert*-butyl perbenzoate, it is possible to calculate $k^\circ_{het} = 2 \times 10^{-9}$ cm s^{-1} and $Z'_{het} = 8$ cm s^{-1}. Very recently, Workentin and co-workers reported evidence indicating that the DET to endoperoxides artemisinin, ascaridole, and dihydroascaridole is nonadiabatic.[36] Therefore, it appears that the homogeneous or heterogeneous DET to peroxides is, as a rule, inherently nonadiabatic. Although for the peresters investigated here the decrease of the preexponential factors with respect to the corresponding adiabatic values may be easily in error by 1 order of magnitude (because of the uncertainty associated with the ΔG° and $\Delta G_0^{\neq}$ estimates), analysis of the reduction results provides compelling evidence for the slowest DET so far characterized.[37]

(30) Rüchardt, C.; Hamprecht, G. *Chem. Ber.* **1968**, 101, 3957.

(31) Crisma, M.; Antonello, S.; Formaggio, F.; Moretto, A.; Maran, F.; Toniolo, C. Work in progress.

(32) X-ray crystallography indicated that **1b** has a *cis*(cyclohexane)−equatorial(phthalimido)−axial(perester) conformation. Full details of the structural analysis of **1b** and related compounds will be published elsewhere.[31]

(33) Valle, G.; Toniolo, C.; Jung, G. *Liebigs Ann. Chem.* **1986**, 1809.

(34) (a) German, E. D.; Kuznetsov, A. M. *J. Phys. Chem.* **1994**, *98*, 6120. (b) German, E. D.; Kuznetsov, A. M.; Tikhomirov, V. A. *J. Phys. Chem.* **1995**, *99*, 9095.

(35) Newton, M. D.; Sutin, N. *Annu. Rev. Phys. Chem.* **1984**, *35*, 437.

(36) (a) Magri, D. C.; Donkers, R. L.; Workentin, M. S. *J. Photochem. Phytobiol. A: Chem.* **2001**, *138*, 29. (b) Donkers, R. L.; Workentin, M. S. *Chem. Eur. J.*, in press.

Intrinsic nonadiabaticity can be confirmed also by carrying out the calculation of the electronic coupling matrix element H_{RP}, along lines similar to those previously described in detail for the intermolecular DET to dialkyl peroxides.[11] Thus, we used the German−Kuznetsov nonadiabatic DET theory in its semiclassical limit, in which the intramolecular modes and the solvent polarization are treated classically (harmonic approximation).[34] A Morse potential was used for the motion along the O−O bond coordinate, whereas the energy curve of the fragmented products was taken as the repulsive part of the reactant Morse curve, as in the original Savéant theory.[17] Under these conditions, the rate constant for DET between donor and acceptor at encounter distance ($k^{\neq}$) can be expressed by eq 8 in

$$k^{\neq} = \frac{2\pi}{\hbar}(H_{RP})^2\{16\pi RT\Delta G_0^{\neq}\exp[-\beta(r^{\neq} - r_0)]\}^{-1/2} \exp(-\Delta G^{\neq}/RT) \quad (8)$$

which $r^{\neq} - r_0$ is the bond elongation at the transition state, β is the Morse exponential factor, and $\Delta G^{\neq}$ is the activation free energy. Therefore, H_{RP} can be calculated once the first-order rate constant $k^{\neq}$ is related to the experimental rate constant k_{inter} and all the other quantities on the right-hand side of eq 8 are calculated. k_{inter} can be corrected to $k^{\neq}$ by using the equilibrium constant (K_d) for the diffusion-controlled formation of reacting D/A complex, i.e., $k_{inter} = K_d k^{\neq}$. To calculate K_d, we used equation $K_d = [(4\pi N r^2 \delta r)/1000]$,[38] which takes into account that the peroxide acceptor is uncharged and thus that no electric work is required to form the encounter complex. According to this model, the DET is viewed as occurring significantly only between the contact distance r (taken as the van der Waals distance $r_D + r_A$) and $r + \delta r$, in which δr ranges from ∼2 to ∼0.3 Å for adiabatic and nonadiabatic reactions, respectively.[38] β, 2.84 Å^{-1}, was calculated from the O−O stretching frequency ν_0[39] using the relationship $\beta = \nu_0(2\pi^2\mu/\mathrm{BDE})^{1/2}$, where μ is the reduced mass. The bond elongation $r^{\neq} - r_0$ is related to the reaction free energy $\Delta G°$[34] and becomes larger for less exoergonic reactions. Because of the weakness of the perester O−O bond, $r^{\neq} - r_0$ is rather small. In particular, we estimated that $r^{\neq} - r_0$ ranges from 0.09 to 0.17 Å for $\Delta G° = -1.11$ and -0.50 eV, respectively. $\Delta G^{\neq}$, $\Delta G_0^{\neq}$, and $\Delta G°$ were calculated as already described. By using this procedure, we found that for the homogeneous reduction of **2a** H_{RP} is indeed remarkably small, being in the range 0.1−0.3 cm^{-1} throughout the series of mediators employed. As for the Z' estimates, these H_{RP} values also suffer from the uncertainty of the input estimated quantities and the limits of the theory. Nevertheless, it is interesting to observe that the calculated H_{RP} values correspond to a rate drop of ∼6 orders of magnitude with respect to an adiabatic process.

An aspect that is particularly worth noting about the present investigation is that the same nonadiabaticity outcome could be observed by using electrode, solution, or intramolecular donors. This implies that the D/A orientation cannot be an important issue because both the heterogeneous and the homogeneous intermolecular DET rates are the result of random distance and orientation distributions between D and A. In keeping with this reasoning, it thus appears that there should be an intrinsic reason for observing such a slow DET rate. Very recently, it has been argued on the basis of both experimental data and theoretical calculations that there are reactions whose rate is markedly reduced because of the failure of the Born−Oppenheimer approximation near the transition state; a very nice and mind-provoking account on the matter has been published very recently by Butler, who contributed significantly to this topic.[40] In these reactions, such as for example some photodissociations, the electronic wave function does not instantaneously adjust along the reaction coordinate near the transition state. In fact, the dominant bonding electronic configuration on the reactant side must change to become repulsive past the transition state. If the dynamics of the electronic rearrangement is sufficiently slow, the crossing between the reactant and product curves is only narrowly avoided, causing the reaction rate to drop significantly. An analogous situation may hold for concerted DETs, in which the donor injects one electron into the σ^* orbital of the frangible bond. In this framework, it would not be unreasonable to start considering DETs as reactions that are particularly susceptible to proceed nonadiabatically. This hypothesis, however, calls for theoretical and further experimental studies.

By taking into account the present results as well as those obtained previously with other dissociative-type acceptors, it also appears that the weaker the cleaving bond the smaller the electronic coupling matrix element H_{RP}. In fact, the BDE and average H_{RP} values (the comparison is for $\delta r = 0.3$ Å) are as follows: *tert*-butyl bromide, 66 kcal mol^{-1} and 190 cm^{-1}; di-*tert*-butyl peroxide, 37.3 kcal mol^{-1} and 15 cm^{-1}; dicumyl peroxide, 36.2 kcal mol^{-1} and 17 cm^{-1};[11] **2a**, 30.6 kcal mol^{-1} and 0.3 cm^{-1}. On the other hand, within the description of the reactant and product energy curves in terms of the Morse equation, it is worth reminding that, for a given cleaving bond, stretching frequency ν_0, and $\Delta G°$, bond elongation at the transition state is minimized by a decrease of BDE. On these grounds, one might be tempted to speculate that a more reactant-like transition state also implies a larger degree of electronic wave function reorganization. It follows that lowering the driving force would increase the electronic coupling between the reactant and product energy curves at the transition state and thus the DET rate. In keeping with this hypothesis, we note that for the nonadiabatic reduction of di-*tert*-butyl peroxide the Arrhenius preexponential factor (which is proportional to H_{RP}^2, as shown in eq 8) indeed increases as the driving force decreases.[11] A similar, although less pronounced trend, was reported in the temperature study of the reduction of *tert*-butyl bromide by aromatic radical anions.[41a] The trend observed with other halides, however, led to ambiguous results.[41] On the other hand, we expect that nonadiabatic rather than intrinsically fast DETs would be more prone to be affected by this rate-enhancing mechanism at low driving forces. This is an intriguing possibility that would suggest a new way of looking at the long-debated problem of why some DET systems give rise to almost linear activation/driving force relationships.[42,43]

It is evident that the nonadiabatic issue is at its very beginning in the area of DETs. More experimental data on carefully selected acceptor molecules and specific theoretical calculations are definitely needed to better understand the reasons why some

(37) Nonadiabaticity cannot be attributed to steric hindrance; as a matter of fact, we showed that screening of the O−O σ^* orbital by the bulky *tert*-butyl groups of di-*tert*-butyl peroxide is responsible for a rate drop of only 0.8 log unit.[11]

(38) Sutin, N. *Prog. Inorg. Chem.* **1983**, *30*, 441.

(39) Our own measurements led to 854 cm^{-1}, a value that is within the very narrow range of frequencies reported for the O−O vibration of an extensive series of peroxides: Vacque, V.; Sombret, B.; Huvenne, J. P.; Legrand, P.; Suc, S. *Spectrochim. Acta A* **1997**, *53*, 55.

(40) See: Butler, L. J. *Annu. Rev. Phys. Chem.* **1998**, *49*, 125 and pertinent references therein.

(41) (a) Daasbjerg, K.; Pedersen, S. U.; Lund, H. *Acta Chem. Scand.* **1991**, *45*, 424. (b) Balslev, H.; Daasbjerg, K.; Lund, H. *Acta Chem. Scand.* **1993**, *47*, 1221.

(42) (a) Lund, H.; Daasbjerg, K.; Lund, L.; Pedersen, S. U. *Acc. Chem. Res.* **1995**, *28*, 313. (b) Lund, H.; Daasbjerg, K.; Lund, T.; Occhialini, D.; Pedersen, S. U. *Acta Chem. Scand.* **1997**, *51*, 135.

of these DET reactions are inherently very slow. Most probably, the study of intramolecular DET rates in well-defined D-Sp-A molecules will provide a particularly efficient tool to gain new insights into the fine details of the dynamics of these dissociative processes.

Experimental Section

Synthesis and Characterization. Melting points were determined using a Leitz model Laborlux 12 apparatus and are not corrected. Thin-layer chromatography (TLC) and column chromatography were performed on Merck Kieselgel 60 F_{254} plates and on Merck Kieselgel 60 (0.040−0.063 mm), respectively. The following eluants were used for TLC analysis: (1) chloroform−ethanol, 9:1; (2) toluene−ethanol, 7:1; (3) ethyl acetate−petroleum ether, 1:8; (4) 1-butanol−acetic acid−water, 3:1:1. The TLC chromatograms were visualized by UV fluorescence (254 nm) or developed by chlorine−starch−potassium iodide chromatic reaction, as appropriate. Selective visualization of the −O−O− bond was achieved by developing the TLC plates with a solution of NH_4SCN (0.63 g) and $FeSO_4{\cdot}(NH_4)_2SO_4{\cdot}6H_2O$ (Mohr's salt, 0.88 g) in 1% H_2SO_4 (12 mL). All compounds were obtained in a chromatographically homogeneous state. The solid-state IR absorption spectra (KBr disk technique) were recorded with a Perkin-Elmer model 1720X FT-IR spectrophotometer, nitrogen-flushed, equipped with a sample shuttle device, at 2-cm^{-1} nominal resolution, averaging 50 scans. ^1H NMR and ^{13}C NMR spectra were obtained by using a Bruker model AC 250 spectrometer. Deuteriochloroform (99.96%, *d*; Aldrich) and deuterated dimethyl sulfoxide (99.96%, d_6; Acros Organics), with tetramethylsilane as the internal standard, were used as solvents.

The mixed alkyl−acyl peroxides (peresters) **2a**[21a] and **2b**[44] were prepared by using a literature procedure.[45] The mediators used for the homogeneous redox catalysis experiments were commercially available or synthesized as described below.

Pht-Aib-OO*t*Bu (1a) (Pht, phthaloyl; Aib, α-aminoisobutyric acid).[30] With respect to the previously described literature procedure,[30] an improved synthetic protocol was employed. To an ice-cold solution of Pht-Aib-OH[30] (0.40 g, 1.6 mmol) in CH_2Cl_2 (6 mL), 4-(dimethylamino)-pyridine (DMAP; 0.20 g, 1.6 mmol) and *N*-ethyl-*N*′-dimethylaminopropylcarbodiimide) hydrochloride (EDC; 0.31 g, 1.6 mmol) were added, followed by a 5.5 M solution of *tert*-butyl hydroperoxide in *n*-decane (0.29 mL, 1.6 mmol). After stirring for 4 h at room temperature, the reaction mixture was evaporated to dryness and the residue dissolved in ethyl acetate (EtOAc). The organic solution was washed with 10% $KHSO_4$, H_2O, 5% $NaHCO_3$ and H_2O, dried over Na_2SO_4, and evaporated to dryness. The title compound was purified by silica gel column chromatography (EtOAc−petroleum ether 1:8). It precipitated as a waxy solid from a EtOAc solution upon addition of petroleum ether. Yield, 80%: $R_{f1} = 0.95$; $R_{f2} = 0.95$; $R_{f3} = 0.35$; IR (KBr) 1780, 1719 cm^{-1}; ^1H NMR ($CDCl_3$) δ 7.83 and 7.73 (2m, 4H, Pht CH), 1.91 (s, 6H, Aib CH_3), 1.34 (s, 9H, OO*t*Bu CH_3);^{13}C NMR ($CDCl_3$) δ 169.98 (perester CO), 167.96 (Pht CO), 134.14 (phenyl CH^4 and CH^5), 131.65 (phenyl CH^1 and CH^2), 123.18 (phenyl CH^3 and CH^6), 84.33 (OO*t*Bu quaternary C), 60.25 (Aib quaternary C), 26.14 (OO*t*Bu CH_3), 24.67 (Aib CH_3).

***cis*-4-Phthaloylaminocyclohexanecarboxylic Acid.** $(Pht)_2O$ (0.26 g, 2.5 mmol) and *cis*-4-aminocyclohexanecarboxylic acid (0.30 g, 2.1 mmol) were finely ground and then melted at 190 °C. After 15 min, heating was stopped. The cold reaction mixture was dissolved in a H_2O−triethylamine (pH 8) solution and extracted with diethyl ether. The aqueous layer was acidified to pH 2 with $KHSO_4$ and extracted twice with EtOAc. The organic phase was washed with H_2O, dried over Na_2SO_4, and evaporated to dryness. From this residue, the title compound was isolated by flash chromatography (CH_2Cl_2−EtOH 96:4). Yield, 90%: mp 191−192 °C (EtOAc−petroleum ether); $R_{f1} = 0.80$; $R_{f2} = 0.55$; $R_{f4} = 0.80$; IR (KBr) 1773, 1704 cm^{-1}; ^1H NMR (DMSO-d_6) δ 7.83 (s, 4H, Pht CH), 3.90 (m, 1H, cyclohexane CH), 2.6 (m, 1H, cyclohexane CH), 2.20 (m, 4H, cyclohexane CH_2), 1.55 (m, 4H, cyclohexane CH_2).

***cis*-4-Phthaloylaminocyclohexanecarboxylic Acid-OO*t*Bu (1b).** This compound was prepared from *cis*-4-phthaloylaminocyclohexanecarboxylic acid (0.15 g, 0.55 mmol) and a 5.5 M solution of *tert*-butyl hydroperoxide in *n*-decane (0.10 mL, 0.55 mmol) as described above for **1a** and purified by flash chromatography (EtOAc−petroleum ether 1:9). Yield, 79%: mp 105−106 °C (EtOAc−petroleum ether); $R_{f1} = 0.95$; $R_{f2} = 0.95$; $R_{f3} = 0.30$; IR (KBr) 1769, 1723, 1703 cm^{-1};^1H NMR ($CDCl_3$) δ 7.78 and 7.67 (2m, 4H, Pht CH), 4.15 (m, 1H, cyclohexane CH), 2.85 (m, 1H, cyclohexane CH), 2.50 (m, 4H, cyclohexane CH_2), 1.70 (m, 4H, cyclohexane CH_2), 1.38 (s, 9H, OO*t*Bu CH_3); ^{13}C NMR ($CDCl_3$) δ 171.13 (perester CO), 168.06 (Pht CO), 133.76 (phenyl CH^4 and CH^5), 131.95 (phenyl CH^1 and CH^2), 123.02 (phenyl CH^3 and CH^6), 83.48 (OO*t*Bu quaternary C), 50.10, 36.84, 26.95, 26.41, 26.24 (cyclohexane CH and CH_2 and OO*t*Bu CH_3).

Pht-Aib-OMe (3a). To an ice-cold solution of Pht-Aib-OH (1 g, 4.2 mmol) in CH_2Cl_2 (10 mL), DMAP (0.5 g, 4.2 mmol) and EDC·HCl (0.79 g, 4.2 mmol) were added, followed by methanol (0.17 mL, 4.2 mmol). After stirring for 4 h at room temperature, the reaction mixture was evaporated to dryness and the residue dissolved in EtOAc. The organic solution was washed with 10% $KHSO_4$, H_2O, 5% $NaHCO_3$, and H_2O, dried over Na_2SO_4, and concentrated under reduced pressure. A flash chromatography step (CH_2Cl_2−EtOH 98:2) was required to purify the title compound. Yield, 80%: mp 70 °C (EtOAc−petroleum ether); $R_{f1} = 0.90$; $R_{f2} = 0.90$; $R_{f3} = 0.30$; IR (KBr) 1765, 1734, 1710 cm^{-1}; ^1H NMR ($CDCl_3$) δ 7.80 and 7.70 (2m, 4H, Pht CH), 3.75 (s, 3H, OMe CH_3), 1.85 (s, 6H, Aib CH_3).

3-FPht-Aib-OH (3-FPht, 3-fluorophthaloyl). This derivative was prepared from H-Aib-OH (0.46 g, 4.5 mmol) and the symmetrical anhydride $(3\text{-FPht})_2O$ (1 g, 5.4 mmol) according to the procedure described for Pht-Aib-OH.[30] Yield, 79%: mp 145−146 °C (EtOAc−petroleum ether); $R_{f1} = 0.75$; $R_{f2} = 0.50$; $R_{f4} = 0.80$; IR (KBr) 1785, 1717 cm^{-1}; ^1H NMR ($CDCl_3$) δ 7.70 and 7.35 (2m, 3H, Pht CH), 1.87 (s, 6H, Aib CH_3).

3-FPht-Aib-OMe. This derivative was prepared from 3-FPht-Aib-OH (1 g, 4.0 mmol) as described above for Pht-Aib-OMe. Yield 76%: mp 95−96 °C (EtOAc−petroleum ether); $R_{f1} = 0.90$; $R_{f2} = 0.90$; $R_{f3} = 0.35$; IR (KBr) 1776, 1736, 1710 cm^{-1}; ^1H NMR ($CDCl_3$) δ 7.80 and 7.36 (2m, 3H, Pht CH), 3.76 (s, 3H, OMe CH_3), 1.83 (s, 6H, Aib CH_3).

***cis*-4-Phthaloylaminocyclohexanecarboxylic Acid-OMe (3b).** This compound was prepared from *cis*-4-phthaloylaminocyclohexanecarboxylic acid (0.10 g, 0.37 mmol) as described above for **3a** and purified by flash chromatography (CH_2Cl_2−EtOH 97:3). Yield, 88%: mp 128−129 °C (EtOAc−petroleum ether); $R_{f1} = 0.90$; $R_{f2} = 0.90$; $R_{f3} = 0.30$; IR (KBr) 1765, 1723, 1706 cm^{-1};^1H NMR ($CDCl_3$) δ 7.80 and 7.70 (2m, 4H, Pht CH), 4.15 (m, 1H, cyclohexane CH), 3.76 (s, 3H, OMe CH_3), 2.65 (m, 1H, cyclohexane CH), 2.3 (m, 4H, cyclohexane CH_2), 1.65 (m, 4H, cyclohexane CH_2).

Electrochemical Apparatus and Procedures. *N*,*N*-Dimethylformamide (Carlo Erba, 99.8%) and tetrabutylammonium perchlorate (Fluka, 99%) were treated as previously described.[13] Electrochemical measurements were conducted in an all-glass cell, thermostated at the required temperature. An EG&G-PARC 173/179 potentiostat−digital coulometer, EG&G-PARC 175 universal programmer, Nicolet 3091 12-bit resolution digital oscilloscope, and Amel 863 X/Y pen recorder were used. The feedback correction was applied to minimize the ohmic drop between the working and the reference electrodes. The glassy carbon (Tokai GC-20) electrode was prepared and activated before each measurement as previously described.[13] The electrode area was determined through the limiting convolution current of ferrocene, the diffusion coefficient of ferrocene being 1.13×10^{-5} cm^2 s^{-1} in DMF.[11] Some experiments were carried out on **3a** by using a mercury microelectrode.[13] The reference electrode was Ag/AgCl, calibrated after each experiment against the ferrocene/ferricenium couple. In the presence of 0.1 M TBAP, we measured $E°_{Fc/Fc+}$ to be 0.464 V versus

(43) Other mechanisms have been proposed to be responsible for rate enhancement at low driving forces. One of them considers the interference of an inner-sphere component when the ET becomes more endergonic.[42] Recently, Jensen and Daasbjerg published very interesting results suggesting that for some halides the rate could be enhanced at low driving forces because of a more pronounced S_N1-like contribution to the transition-state structure (Jensen, H. K.; Daasbjerg, K. *J. Chem. Soc., Perkin Trans 2* **2000**, 1251.).

(44) Lorenz, P.; Rüchardt, C.; Schacht, E. *Chem. Ber*. **1971**, 104, 3429.

(45) Blomquist, A. T.; Berstein, J. *J. Am. Chem. Soc.* **1951**, *73*, 5546.

the KCl saturated calomel electrode (SCE) in DMF. All potential values are reported versus SCE. The counter electrode was a 1-cm^2 Pt plate.

Convolution and voltammetric analyses were carried out on low-noise voltammetric curves obtained in the range 0.1−50 V s^{-1}, according to a procedure previously described.[13] Since the reduction of peresters, RCO_3tBu, eventually yields RCO_2^- and tBuO$^-$, a small amount of a weak acid, acetanilide, was added to the solution to protonate tBuO$^-$. Acid addition hampered the father−son reaction $RCO_3tBu + t\text{BuO}^- \rightarrow RCO_2tBu + t\text{BuO}_2^-$, which would have affected the voltammetric curves at low scan rate values.[12] The curves were digitalized, corrected for the background contribution by subtracting the curves previously obtained in the absence of the substrate, and then analyzed by using our homemade convolution software or compared with the corresponding digital simulations. The DigiSim 3.03 package was used for all simulations, using a step size of 1 mV and an exponential expansion factor of 0.5.

Acknowledgment. This work was financially supported by the University of Padova (research project A.0EE00.97) and the Ministero dell′Università e della Ricerca Scientifica e Tecnologica (MURST).

JA010799U